Mn5Ge3C0.6/Ge(111) Schottky contacts tuned by a n-type ultra-shallow doping layer

Matthieu Petit, Ryoma Hayakawa, Yutaka Wakayama, Vinh Le Thanh, Lisa Michez

$Mn_5Ge_3C_{0.6}$/Ge(111) Schottky contacts tuned by a n-type ultra-shallow doping layer

Matthieu Petit[1], Ryoma Hayakawa[2], Yutaka Wakayama[2], Vinh Le Thanh[1], Lisa Michez[1]

[1] Aix-Marseille Université, CNRS, CINaM UMR 7325, 13288, Marseille, France
[2] International Center for Materials Nanoarchitectonics (WPI-MANA), National Institute for Materials Science, 1-1 Namiki, Tsukuba 305-0044, Japan

E-mail: matthieu.petit@univ-amu.fr

Abstract. $Mn_5Ge_3C_x$compound is of great interest for spintronics applications. The various parameters of Au/$Mn_5Ge_3C_{0.6}$/Ge(111) and Au/$Mn_5Ge_3C_{0.6}$/δ-doped Ge(111) Schottky diodes were measured in the temperature range of 30-300 K by using current-voltage and capacitance-voltage techniques. The Schottky barrier heights and ideality factors were found to be temperature dependent. These anomaly behaviours were explained by Schottky barriers inhomogeneities and interpreted by means of Gaussian distributions model of the Schottky barrier heights. Following this approach we show that the $Mn_5Ge_3C_{0.6}$/Ge contact is described with a single Gaussian distribution and a conduction mechanism mainly based on the thermoionic emission. On the other hand the $Mn_5Ge_3C_{0.6}$/δ-doped Ge contact is depicted with two Gaussian distributions according to the temperature and a thermionic-field emission process. The differences between the two types of contacts are discussed according to the distinctive features of the growth of heavily doped germanium thin films.

PACS numbers: 73.30.+y, 61.72.uf, 61.72.uj, 73.40.-c, 73.40.Gk, 85.75.-d

Keywords: Mn_5Ge_3, Mn_5Ge_3C, Germanium, δ-doping, Schottky diodes, Schottky barrier anomalies, Spin injection, Molecular beam epitaxy, Reactive deposition epitaxy

1. Introduction

The rapid evolution of electronics results partly in scaling down the device size. But as device miniaturization reaches technological limits, alternative technologies need to be developed and electronics based on the control and the manipulation of spin degree of freedom of charge carriers in semiconductors holds great promises. This new kind of electronics requires an efficient electrical injection of spin-polarized electrons from a ferromagnet into the conduction band of a semiconductor as well as a subsequent spin-polarized detection. Therefore developing suitable materials for electrical spin injection in group-IV semiconductors is a key step toward the full integration of spintronic devices into the semiconductor technology as pinpointed by the International Technology Roadmap for Semiconductor in the "Emerging Research Materials Difficult Challenges 2013-2020" [1].

Two main ways have been explored in order to inject spin-polarized current into silicon or germanium. Firstly, ferromagnetic metal (FM) such as Co, Fe or Ni have been considered. Spin-polarized carriers tunnel from the metal to the semiconductor through an insulator or a Schottky barrier [2]. However most ferromagnetic metals react with Si and Ge to form non-ferromagnetic interfacial silicides or germanides. It is also not trivial to obtain epitaxial growth of an oxide between Ge (or Si) and a ferromagnetic metal. The other possibility is to use heterostructures of semiconductors and ferromagnetic semiconductors. But to date no semiconductor showing a ferromagnetic order up to room temperature can be obtained in a reproducible manner.

In this context, Mn_5Ge_3 and Ge are potentially interesting. First of all, Ge is gaining a strong interest in the spintronics field due to its large spin diffusion length and its high carrier mobility. Despite a strong Fermi level pinning (FLP) in metal/Ge contacts [3], electrical spin injection has been demonstrated in Ge with the use of a metal electrode and an oxide tunnel barrier [4, 5, 6, 7]. Moreover, Yamane *et al.* recently demonstrated in the Fe_3Si/Ge(111) system that the FLP effect can be reduced thanks to a high quality structure with an atomically flat interface and they attributed the magnitude of the FLP effect to the presence of disorder at the metal/Ge interface [8]. This underlines the need of a very well controlled and clean interface. Then Mn_5Ge_3 is an intermetallic compound that can be grown epitaxially on Ge(111) [9, 10]. Its Curie temperature is about 296 K and can be enhanced by carbon doping up to 430 K [11, 12] for $Mn_5Ge_3C_{0.6}$. Recently, there have been studies from several teams on the Mn_5Ge_3/Ge(111) contact [13, 14, 15, 16] and specially a report has been published on a large spin accumulation voltage in Mn_5Ge_3/Ge(111) without an oxide tunnel barrier [17].

Generally speaking, Schottky contacts can be tailored using interfacial layers engineering [18, 19, 20]. More specifically, the Schottky contacts between a ferromagnet electrode and a semiconductor can be tuned by playing with the doping profile at the interface [21]. According to Albrecht *et al.*, the spin injection is deteriorated by the depletion region but can be tailored by a heavily doped layer such as a δ-doped layer [22]. The Schottky barrier parameters i.e. barrier height, depletion region width and contact resistance, are then reduced. Sawano *et al.* have shown that the contact resistance in a Fe_3Si/Ge(111) structure can be substantially reduced when a control Sb δ-doping is introduced in Ge very close to the interface [23] and the combination of high quality Schottky tunnel barrier contact and surface doped layer has led to successful spin accumulation in Fe_3Si/Ge(111) [24].

In this framework, we have studied the features of the Au/$Mn_5Ge_3C_{0.6}$/Ge(111) Schottky contacts by intensity-voltage-temperature (I-V-T) and capacitance-voltage-temperature (C-V-T) electrical measurements, $Mn_5Ge_3C_{0.6}$ presenting the highest Curie temperature of the $Mn_5Ge_3C_x$ alloys. The $Mn_5Ge_3C_{0.6}$ thin films were grown by an uncommon growth process (low temperature reactive deposition epitaxy so-called RDE) we recently developed to improve the quality of the $Mn_5Ge_3C_x$/Ge(111) interfaces [25]. Furthermore, we concurrently investigated the effect of a heavily n-type δ-doped layer on the interfacial characteristics of Au/$Mn_5Ge_3C_{0.6}$/Ge(111) Schottky contacts, since such a very thin layer can be a tool to modify these key characteristics regarding the spin injection.

2. Experimental details, devices fabrication and characterisation

Two types of samples were prepared with the following structures (fig.1) from top to bottom: the top contacts are made of a 3 nm Cr bond coat followed by a 100 nm Au layer patterned in 100 $\times$ 100 μm^2 squares by optical lithography. The contacts size was chosen to avoid edge effects.

The $Mn_5Ge_3C_{0.6}$ thin films growth on Ge(111) was performed using the RDE method at room temperature. This method has been described and characterised elsewhere and involves the co-deposition of Ge, Mn and C atoms on Ge(111) surface at room temperature [25, 26]. It ensures a very high crystalline quality of the $Mn_5Ge_3C_x$ thin films and a

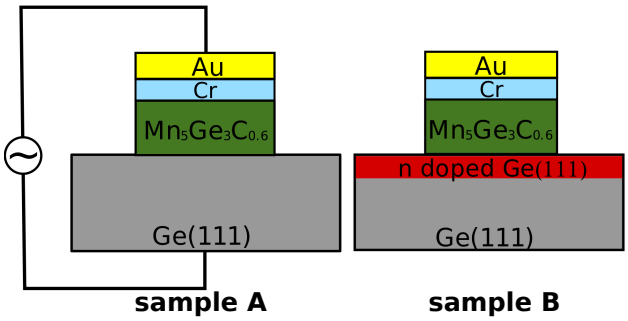

Figure 1. Drawings of the investigated Schottky diodes with the P δ-doped layer on the right and without on the left.

sharp interface between these films and the Ge(111) substrates. The n-type Ge(111) substrates are from UMICORE with a resistivity of 1.5 $\Omega.cm^{-1}$ (doping concentration in the order of 10^{15} cm^{-3}). On one sample a heavily n-type δ-doped layer was inserted at the top of the Ge(111) substrates prior to the deposition of the $Mn_5Ge_3C_{0.6}$ thin films (sample B). The target doping concentration of this δ-doped layer is 2×10^{19} cm^{-3}. The layer is grown by a co-deposition of Ge evaporated from a two-zone heated Knudsen effusion cell and phosphorous atoms produced by a GaP decomposition source (DECO fom Dr. Eberl MBE-Komponenten GmbH). The growth parameters required to reach the high doping concentration were optimized in a previous work [27]. The Schottky diodes properties were measured with a semiconductor device analyser (Agilent B1500A) in a vacuum chamber at 10^{-2} Pa over a temperature range of 30-300 K through a helium-based closed cycle refrigeration system.

3. Results and discussion

3.1. Extraction of Schottky diodes parameters

The forward I-V characteristics displayed on fig.2a) and b) show typical examples of experimental measurements obtained on the $Au/Mn_5Ge_3C_{0.6}$ diodes respectively without and with the presence of a n-type δ doped layer.

A gradual shift of the I-V curves towards higher voltages is observed with the decrease of the temperature for both samples. This indicates that the transport mechanism is thermally assisted and not pure tunnelling. This thermally assisted transport was observed in previous studies of $Mn_5Ge_3/Ge(111)$ Schottky contacts without carbon doping [15, 17, 28]. On fig.2b) two behaviours can be clearly seen through the two linear regions with different slopes of the semi-logarithmic curves. This point will be discussed later. An example of C-V measurements from both samples is given in fig.2c) at one temperature for clarity. From

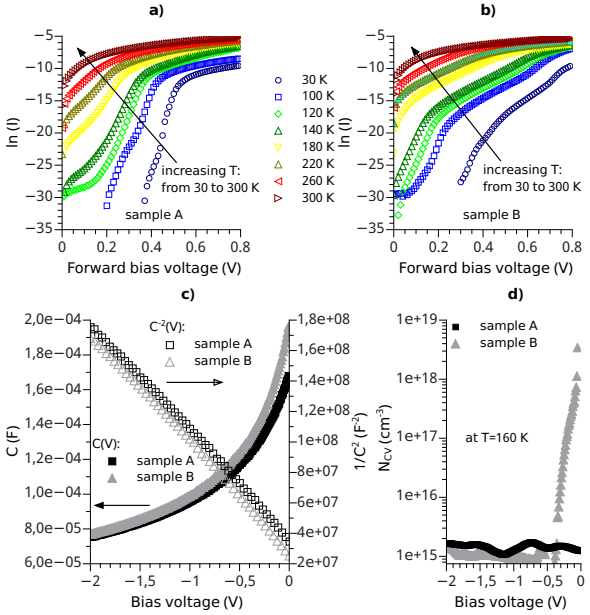

Figure 2. a) and b) typical forward current-voltage characteristics for Schottky diodes without (sample A) and with (sample B) a δ-doped layer, c) C-V and $1/C^2$-V typical plots at 160 K and 1 MHz and d) corresponding numerically extracted capacitance-voltage profiles N_{CV}.

these measurements we extracted numerically the C-V profiles N_{CV} (eq.1) so as to get a confirmation on an electrical level of the effect of the δ doped layer [29, 30]:

$$N_{CV} = \frac{C^3}{q\epsilon_s}\frac{dV}{dC} \quad (1)$$

where q is the electron charge and ϵ_s the permittivity of the semiconductor. The sample without the δ-layer presents a rather flat profile with an mean value of about 1.4×10^{15} cm^{-3} consistent with the manufacturer specifications of the Ge wafer and the sample with the δ doped layer exhibits the same flat profile except near the interface where the doping concentration increases to about 3×10^{18} cm^{-3}. This is in agreement with our previous results and the consideration on the difference between dopant concentrations evaluated by chemical or electrical measurements [27, 31].

To begin our analyses on the Schottky contacts we assumed a thermoionic emission (TE) conduction mechanism expressed by the following equation [32]:

$$I = I_s\left\{exp\left[\frac{q\,(V - IR_s)}{nk_BT}\right] - 1\right\} \quad (2)$$

where k_B the Boltzmann constant, n the ideality factor, R_s is the series resistance and I_s the saturation current which is given by:

$$I_s = \mathcal{A}A^*T^2exp\left(-\frac{q\Phi_{IV}}{k_BT}\right) \quad (3)$$

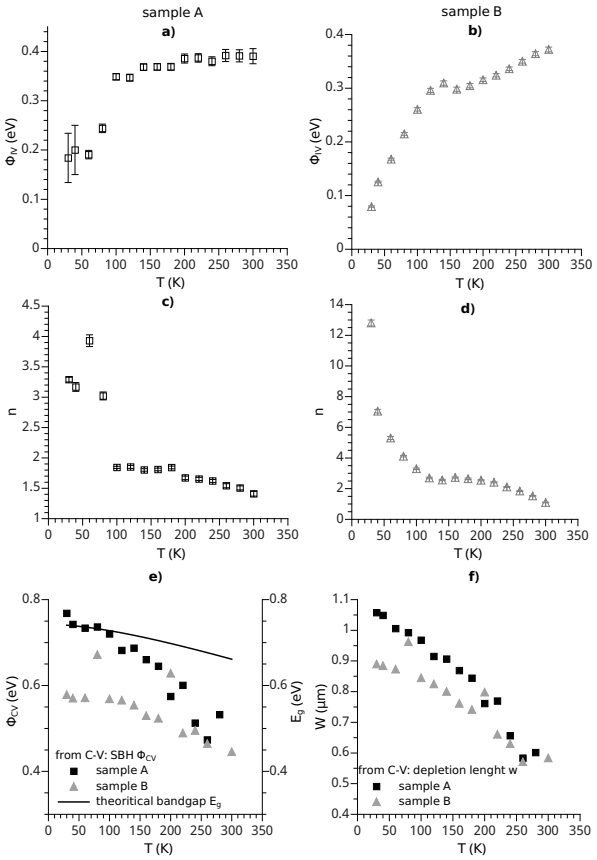

Figure 3. a) and b) Schottky barrier heights Φ_{IV} of the samples without (A) and with (B) a δ-doped layer respectively, c) and d) ideality factors n from the I-V measurements. e) Schottky barrier heights Φ_{CV} from the C-V measurements and f) depletion length W in micrometer calculated from the C-V curves on samples without and with a δ-doped layer.

$\mathcal{A}$ is the diode area, A^* is the effective Richardson constant and Φ_{IV} is the zero bias Schottky barrier height (SBH). Several methods can be used to determine the Schottky diode parameters. Based on the review written by Olikh *et al.*, our choice fell on the Gromov method [33, 34]. This method allows to find the parameters by a fitting procedure of the I-V curves. According to this one, R_s varied from 3500 Ω at 30 K to 98 Ω at 300 K for the sample without the δ doped layer and from 330 Ω at 30 K to 125 Ω at 300 K for the sample with the δ-doped layer which is in agreement with the low-resistivity Ohmic contacts obtained by δ-doping technique in ref.[23]. The evolution of Φ_{IV} and the ideality factor n versus temperature is plotted on fig.3 for both sets of sample: without (a) sample A) and with (b) sample B) a δ-doped layer.

These figures show a dependence of Φ_{IV} and n with the temperature especially below 120 K: n decreases with temperature whereas Φ_{IV} increases. The δ-doped layer seems to reduce the value of Φ_{IV} over the whole temperature range and to strongly affect the value of the ideality factor. We have also determined the SBH from the C-V data (Φ_{CV}) by using the $1/C^2$ versus bias voltage graph [35, 32]. Typical examples of such graphs are presented in fig.2c) and show a linear relationship between $1/C^2$ and the applied voltage. The C-V characteristics do not depend on frequency between 10kHz and 1MHz (not shown here) and hysteresis are not observed with forward and reverse bias voltage. Thus there is no significant amount of deep levels within the space charge region [36, 37] and no trapped charge. The values of Φ_{CV} are displayed in fig.3c). We observed a decrease of the SBH with the increase of the temperature in a similar trend of the bandgap (continuous black line on fig.3c) calculated from ref.[38, 39]) unlike Φ_{IV} versus T. Moreover Φ_{CV} of the sample with a δ-doped layer is lower than the sample without and consequently the depletion lengths W inferred from Φ_{CV} in fig.3d) are shorter with the presence of a δ-doped layer in agreement with previous works [22, 23]. This last point is particularly interesting in the context of the spin injection since the depletion region is basically a region of rather high resistivity which has been proved to be detrimental to the spin polarization [22]. The SBH values from this work and literature coming from I-V and C-V are summarized in table 1. Regarding the conflicting behaviour issuing from the evolution of Φ_{IV} and Φ_{CV} versus the temperature, it has been already reported for other metal-semiconductor junctions. The SBH of an ideal metal-semiconductor junction is expecting to decrease with the increase of the temperature. The discrepancy comes from spatially inhomogeneous barriers which can be described by Gaussian or multiple Gaussian distributions of the SBH (as discussed in the next part). These inhomogeneities mainly affect the I-V data that rather probe local electrical properties since the current is impacted by local patches of low and high resistivity, whereas the capacitances of the Schottky contacts depends only on the mean value of the barrier distribution [37, 40, 41].

3.2. Schottky contacts inhomogeneities: temperature dependence of the Schottky diodes parameters

The reliance on temperature of the SBH and ideality factor n is a common "abnormality" - the so-called T_0 anomaly- of the Schottky contacts behaviours which is not described by the TE theory. Many forms of temperature dependence exist and have been reported in literature [37, 40, 42]. These phenomena are explained by SBH inhomogeneities: the contacts between metal and semiconductor are not ideal, which means that there are some unavoidable fluctuations of the SBH on the whole area of the electric contact [43, 44]. The fluctuations can be modelled by several

Table 1. Summary of Schottky barrier parameters extracted from I-V and C-V measurements

	growth methods									
	SPE					RDE				
	Φ_{IV} (eV)		Φ_{CV} (eV)		R_s (Ω)	Φ_{IV} (eV)		Φ_{CV} (eV)		R_s (Ω)
Nature of Schottky contacts	100 K	RT	100 K	RT	RT	100 K	RT	100 K	RT	RT
Mn_5Ge_3/n-Ge(111) [13]		0.30	0.67							
Mn_5Ge_3/n-Ge(111) [15]	0.27	0.55			90					
$Mn_5Ge_3C_{0.6}$/n-Ge(111)						0.35	0.39	0.72	0.73	98
$Mn_5Ge_3C_{0.6}$/n-δ-doped layer/n-Ge(111)						0.26	0.37	0.57	0.45	125

sub-areas having each a barrier height. Thus to go deeper in the analysis of our I-V results, we will consider a multiple Gaussian distribution of the SBH values to describe the spatially inhomogeneities of the Schottky contacts according to the temperature range. The temperature dependence of the barrier height of such contacts is thus written as follow [44, 45, 46, 47]:

$$\Phi_{IV-i} = \overline{\Phi}_{IV-i} - \frac{q\,\sigma_i^2}{2k_BT_i} \tag{4}$$

Here $\overline{\Phi}_{IV-i}$ and σ_i stand for the mean barrier height and standard deviation of each barrier distributions i. The estimations of σ_i are calculated by fitting linearly the plots of Φ_{IV} versus $\frac{q}{2k_BT}$ (not shown here) for the samples with and without the δ-doped layer. The plot of Φ_{IV} versus $\frac{q}{2k_BT}$ of the sample without the δ-doped layer exhibits only one linear region which means that the Schottky contact can be described with only one Gaussian distribution. On the contrary in the case of the sample with the δ-doped layer, the Φ_{IV} versus $\frac{q}{2k_BT}$ plot shows two linear regions transitioning around 120 K. It means that the contact of this sample is characterised with two Gaussian distributions: Φ_{IV} and σ present different values according to the temperature range. The results are displayed on table 2.

Table 2. Results of the linear fits of Φ_{IV} versus $\frac{q}{2k_BT}$ for the samples with and without the δ-doped layer assuming a multi-Gaussian distributions of the SBH. R_i^2 are the correlation coefficients of the fits.

δ-doped layer	without	with
Gaussian distribution 1	whole T range	above 120 K
$\overline{\Phi}_{IV-1}$ (eV)	0.45	0.45
σ_1 (V)	0.050	0.067
R_1^2	0.91	0.94
Gaussian distribution 2		below 120 K
$\overline{\Phi}_{IV-2}$ (eV)	-	0.31
σ_2 (V)	-	0.036
R_2^2		0.95

To check the results of the multi-Gaussian distribution model of the SBH, we look at the Richardson plot (fig.4): the plot $ln\left(I_s/T^2\right) = f\left(1/T\right)$ coming from eq.3 should be linear in the case of an homogeneous Schottky contact. In the case of the Gaussian distributions of the SBH, the linearisation of the Richardson plot is obtained by subtracting $\frac{q^2}{2k_B^2T_i^2}\,\sigma_i^2$ to $ln\left(\frac{I_s}{T_i^2}\right)$ according to the temperature ranges T_i. It gives the following equation:

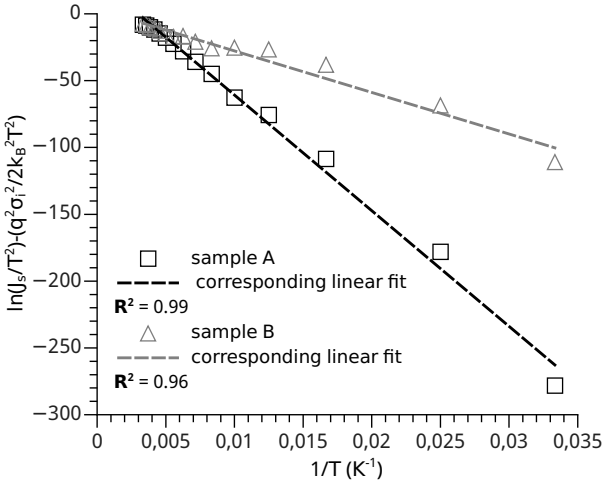

Figure 4. Richardson modified plots and corresponding linear fits for $Mn_5Ge_3C_{0.6}$/Ge(111) Schottky contacts with and without a δ-doped layer according to a multi-Gaussian distributions model of the SBH.

$$ln\left(\frac{I_s}{T_i^2}\right) = lnA^* - \frac{q}{k_BT_i}\,\overline{\Phi}_{IV-i} + \frac{q^2}{2k_B^2T_i^2}\,\sigma_i^2 \tag{5}$$

The good correlation coefficients of the linear fits confirm the validity of the chosen model. To explain the presence of inhomogeneities at the metal-semiconductor interface, we can look into more details the growth process of the $Mn_5Ge_3C_{0.6}$ thin films. We have shown that there is an interfacial layer of about 2-3 nm thick between the Ge(111) substrate and the $Mn_5Ge_3C_{0.6}$ films involved in the stress relaxation of the latter (lattice mismatch between Ge(111) and Mn_5Ge_3 around 3.7 %) [25]. On a magnetic point

of view, this interfacial layer could be related to the ferromagnetic dead layer highlighted in ref.[48]. The properties of this layer are still under investigations and seem to be strongly influenced by the growth conditions [49]. Moreover the difference between the two samples in term of Gaussian distributions (especially below 120K) may arise from the heavily doped phosphorous δ-layer. As we mentioned earlier, this layer is grown by a co-deposition of Ge and P at low substrate temperature (523 K) according to our previous work where we demonstrated that the sticking coefficient of P_2 is the determining parameter to reach a high doping level in Germanium [27]. No thermal annealing were performed right after the growth of the δ-doped layer. Post growth annealing is indeed not compulsory to achieve high activation of dopants [50]. Moreover it allows to avoid any further segregation of phosphorous atoms which may induce additional inhomogeneities at the interface. However P doped Ge films grown at low temperature usually contain a rather high density of point defects such as vacancies and interstitials [51, 52]. The surface segregation of P atoms has been reported in the case of δ-doping with a significant impact on the electrical activation of dopants [31, 50]. So it might be possible that the δ-doped layer presents some amount of these point defects entailing the observed modification in the SBH distributions compared to the sample without this δ-doped layer.

3.3. Temperature dependences and conduction mechanisms

The field emission and thermoionic-field emission are generally considered as the conduction mechanisms ruling the excess current through the Schottky contacts in the highly doped semiconductors. In the present case of a very thin high n-doped layer, the tunnelling conduction has been proved to be dominant in the Fe_3Si/Ge Schottky contact [23]. In order to get an insight in the type of conduction taking place in our devices, we have analysed the T_0 anomaly by drawing the $\frac{nk_BT}{q}$ vs $\frac{k_BT}{q}$ plots for the sample with and without the δ-doped layer (cf. fig.5).

According to these graphs, we have decided to fit the results from the sample without a δ-doped layer with a simple linear relationship as described in the so-called T_0 effect meaning that the conduction mechanism is mainly supported by TE [53, 42]. The SBH inhomogeneities consisting of low and high-SBH contact regions as brought out by the Gaussian distribution explain this behaviour [40]. We should notice that in our case the slope of our fit is slightly higher than unity in contrary of a pure T_0 effect. This is in agreement with the evolution of the ideality factor of this sample: n depends on the temperature from 30 to 120 K and then is almost constant with a value around 3.8 (cf fig.3a)). This sample presents a mixed trend between a temperature independent and greater than unity ideality factor and the T_0 effect behaviours.

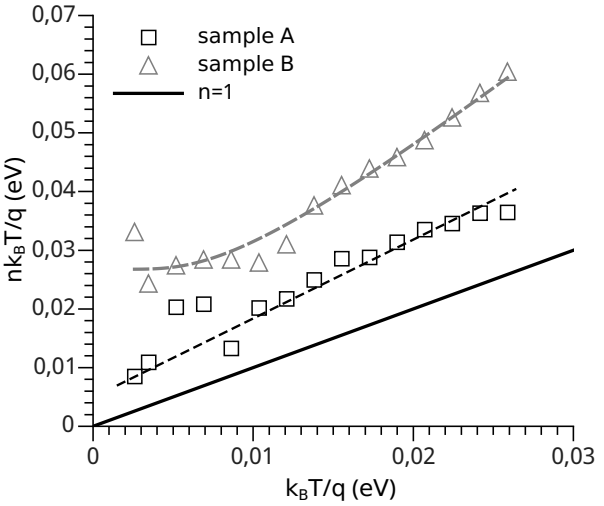

Figure 5. Plots of $\frac{nk_BT}{q}$ vs $\frac{k_BT}{q}$ for the sample with and without the δ-doped layer. The plain dark line corresponds to an ideal Schottky barrier following the TE theory with an ideality factor n=1. The dotted lines correspond to the fits of the experimental data according to the appropriate models (cf. table 3).

Table 3. Results of the fits of the $\frac{nk_BT}{q}$ vs $\frac{k_BT}{q}$ plots of fig.5.

without δ-doped layer	key fitting parameters
without δ-doped layer	linear fit
slope	1.29 ± 0.05
R^2	0.98
with δ-doped layer	$n\frac{k_BT}{q} = \frac{E_{00}}{1-\beta}\, coth\left(\frac{qE_{00}}{k_BT}\right)$
E_{00}	12.6 ± 0.8 meV
R^2	0.96

Regarding the sample with a δ-doped layer, the data were fitted using the TFE model [54, 55]:

$$n\frac{k_BT}{q} = \frac{E_{00}}{1-\beta}\, coth\left(\frac{qE_{00}}{k_BT}\right) \quad (6)$$

In this expression, E_{00} is a characteristic energy of the semiconductor relative to the tunnel effect transmission probability and β is the bias dependence of the barrier height. The theoretical value of E_{00} is given by:

$$E_{00} = \frac{h}{4\pi}\sqrt{\frac{N_D}{m^*\epsilon_s}} \quad (7)$$

where N_D is the free carriers concentration and m^* the effective mass of the free carriers. In our case, this theoretical value is equal to about 7.6 meV.

The results of the fit of the experimental data of fig.5 with eq.6 are given in table 3. The experimental value of E_{00} is higher than the theoretical one. Such an observation was already reported in ref.[55]. A proposed explanation is an increase of the density of states at the metal-semiconductor interface. This is the case in the sample with the δ-doped layer where the interfacial states density N_{ss} is around 5 $\times$ 10^{13} $eV^{-1}.cm^{-2}$ compared to the sample without the doped layer where N_{ss} = 3 $\times$ 10^{12} $eV^{-1}.cm^{-2}$. These comments and the nuances on the relationships between the observed temperature dependence and the TFE mechanism detailed in ref.[40] do not allow to conclude that the TFE theory fully describe the sample with the δ-doped layer. However they are consistent with the presence of low-SBH patches as determined by the Gaussian distributions model of the SBH.

4. Conclusion

The $Mn_5Ge_3C_{0.6}$/Ge and n-δ-doped $Mn_5Ge_3C_{0.6}$/Ge Schottky contacts have been studied as a function of temperature in the range of 30 to 300 K. The $Mn_5Ge_3C_{0.6}$ thin films were grown by a method based on reactive deposition epitaxy recently developed to improve the quality of the interface between Ge(111) and $Mn_5Ge_3C_x$ in the context of the electrical spin injection from $Mn_5Ge_3C_x$ into Ge. The effect of a heavy P δ-doped layer at the interface on the Schottky contact parameters has also been analysed since the use of a δ-doped layer may allow to tune the characteristics of the Schottky contacts. We have shown that the depletion length W is decreased by the added δ-doped layer. This point is interesting for the spin injection. The barrier heights and ideality factors of these $Mn_5Ge_3C_{0.6}$/Ge and δ-doped $Mn_5Ge_3C_{0.6}$/Ge Schottky contacts were found to be temperature dependent. Assuming spatially inhomogeneous contacts, we used a model based on Gaussian distributions of the barrier heights to interpret the experimental data. A deeper analysis of the T_0 anomalies revealed that the $Mn_5Ge_3C_{0.6}$/Ge Schottky contact is mainly controlled by TE conduction and that the δ-doped $Mn_5Ge_3C_{0.6}$/Ge contact may be rather governed by TFE mechanism. These differences between the contacts with and without the δ-doped layer were explained in the light of the growth of this heavy phosphorous doped Ge layer: phosphorous atoms are known to segregate at the surface of the Ge film even at low temperature and then deteriorate the electrical properties of the interface between the metal and the semiconductor. This drawback could be easily overcome by the growth of ultra thin silicon overlayer on top of the δ-doped germanium layer as recently demonstrated in ref.[56] while checking the effect of this extra layer on the spin injection.

Acknowledgements

Parts of this work has been carried out thanks to the support of the A*MIDEX project (ANR-11-IDEX-0001-02) funded by the "Investissements d'Avenir" French Government program, managed by the French National Research Agency (ANR).

References

[1] ITRS 2013 International technology roadmap for semiconductors: emerging research materials summary Tech. rep. ITRS URL http://www.itrs.net/ITRS 1999-2014 Mtgs, Presentations {&} Links/2013ITRS/2013Chapters/2013ERM{_}Summary.pdf

[2] Erve O M J v t, Kioseoglou G, Hanbicki A T, Li C H, Jonker B T, Mallory R, Yasar M and Petrou A 2004 *Applied Physics Letters* **84** 4334 URL http://dx.doi.org/10.1063/1.1758305

[3] Dimoulas A, Tsipas P, Sotiropoulos A and Evangelou E K 2006 *Applied Physics Letters* **89** 252110 URL http://dx.doi.org/10.1063/1.2410241

[4] Liu E S, Nah J, Varahramyan K M and Tutuc E 2010 *Nano Letters* **10** 3297–3301 ISSN 15306984 (*Preprint* 1003.3787) URL http://dx.doi.org/10.1021/nl1008663

[5] Zhou Y, Han W, Chang L T, Xiu F, Wang M, Oehme M, Fischer I, Schulze J, Kawakami R and Wang K 2011 *Physical Review B* **84** 1–7 ISSN 1098-0121 URL http://dx.doi.org/10.1103/PhysRevB.84.125323

[6] Saito H, Watanabe S, Mineno Y, Sharma S, Jansen R, Yuasa S and Ando K 2011 *Solid State Communications* **151** 1159–1161 ISSN 00381098 URL http://dx.doi.org/10.1016/j.ssc.2011.05.010

[7] Jain A, Louahadj L, Peiro J, Le Breton J C, Vergnaud C, Barski A, Beigne C, Notin L, Marty A, Baltz V, Auffret S, Augendre E, Jaffres H, George J M and Jamet M 2011 *Applied Physics Letters* **99** 162102 ISSN 00036951 URL http://dx.doi.org/10.1063/1.3652757

[8] Yamane K, Hamaya K, Ando Y, Enomoto Y, Yamamoto K, Sadoh T and Miyao M 2010 *Applied Physics Letters* **96** 162104 ISSN 00036951 URL http://dx.doi.org/10.1063/1.3368701

[9] Zeng C, Erwin S C, Feldman L C, Li A P, Jin R, Song Y, Thompson J R and Weitering H H 2003 *Applied Physics Letters* **83** 5002–5004 URL http://dx.doi.org/10.1063/1.1633684

[10] Olive-Mendez S F, Spiesser A, Michez L A, Le Thanh V, Glachant A, Derrien J, Devillers T, Barski A and Jamet M 2008 *Thin Solid Films* **517** 191–196 ISSN 0040-6090 URL http://dx.doi.org/10.1016/j.tsf.2008.08.090

[11] Gajdzik M, Sürgers C, Kelemen M T and V Löhneysen H 2000 *Journal of Magnetism and Magnetic Materials* **221** 248–254 ISSN 0304-8853 URL http://dx.doi.org/10.1016/S0304-8853(00)00494-7

[12] Spiesser A, Dau M T, Michez L A, Petit M, Coudreau C, Glachant A and Le Thanh V 2012 *International Journal of Nanotechnology* **9** 428–438 URL http://dx.doi.org/10.1504/IJNT.2012.045346

[13] Nishimura T, Nakatsuka O, Akimoto S, Takeuchi W and Zaima S 2011 *Microelectronic Engineering* **88** 605–609 ISSN 01679317 URL http://dx.doi.org/0.1016/j.mee.2010.08.014

[14] Tang J, Wang C Y, Hung M H, Jiang X, Chang L T, He L, Liu P H, Yang H J, Tuan H Y, Chen L J and Wang K L 2012 *ACS nano* **6** 5710–7 ISSN 1936-086X URL http://dx.doi.org/10.1021/nn301956m

[15] Sellai A, Mesli A, Petit M, Le Thanh V, Taylor D and Henini M 2012 *Semiconductor Science and Technology* **27** 35014 ISSN 0268-1242 URL http://dx.doi.org/10.1088/0268-1242/27/3/035014

[16] Fischer I A, Chang L T, Surgers C, Rolseth E, Reiter S, Stefanov S, Chiussi S, Tang J, Wang K L and Schulze J 2014 *Applied Physics Letters* **105** 3–8 ISSN 00036951 URL http://dx.doi.org/10.1063/1.4903233

[17] Spiesser A, Saito H, Jansen R, Yuasa S and Ando K 2014 *Physical Review B* **90** 1–9 ISSN 1098-0121 URL http://dx.doi.org/10.1103/PhysRevB.90.205213

[18] Ozerden E, Ocak Y S, Tombak A, Kilicoglu T and Turut A 2015 *Thin Solid Films* **597** 14–18 ISSN 00406090 URL http://dx.doi.org/10.1016/j.tsf.2015.11.013

[19] Tanrıkulu E E, Yıldız D E, Günen A and Altındal 2015 *Physica Scripta* **90** 095801 ISSN 0031-8949 URL http://dx.doi.org/10.1088/0031-8949/90/9/095801

[20] Tecimer H, Vural Ö, Kaya A and Altındal 2015 *International Journal of Modern Physics B* **29** 1550076 ISSN 0217-9792 URL http://dx.doi.org/10.1142/S0217979215500769

[21] Pearton S J, Ren F, Abernathy C R, Hobson W S, Chu S N G and Kovalchick J 1989 *Applied Physics Letters* **55** 1342 ISSN 00036951 URL http://dx.doi.org/10.1063/1.101650

[22] Albrecht J D and Smith D L 2003 *Physical Review B* **68** 35340 URL http://dx.doi.org/10.1103/PhysRevB.68.035340

[23] Sawano K, Hoshi Y, Kasahara K, Yamane K, Hamaya K, Miyao M and Shiraki Y 2010 *Journal of Applied Physics* **97** 162108 URL http://dx.doi.org/10.1063/1.3503587

[24] Kasahara K, Baba Y, Yamane K and Ando Y 2012 *Journal of Applied Physics* **111** 07C503 URL http://dx.doi.org/10.1063/1.3670985

[25] Petit M, Michez L, Dutoit C E, Bertaina S, Dolocan V O, Heresanu V, Stoffel M and Le Thanh V 2015 *Thin Solid Films* **589** 427–432 ISSN 00406090 URL http://dx.doi.org/10.1016/j.tsf.2015.05.068

[26] Dutoit C E, Dolocan V O, Kuzmin M, Michez L, Petit M, Le Thanh V, Pigeau B and Bertaina S 2016 *Journal of Physics D: Applied Physics* **49** 45001 ISSN 0022-3727 URL http://dx.doi.org/10.1088/0022-3727/49/4/045001

[27] Luong T K P, Ghrib A, Dau M T, Zrir M A, Stoffel M, Le Thanh V, Daineche R, Le T G, Heresanu V, Abbes O, Petit M, Kurdi M E, Boucaud P, Murota J and Rinnert H 2014 *Thin Solid Films* **557** 70–75 URL http://dx.doi.org/10.1016/j.tsf.2013.11.027

[28] Nishimura T, Kita K and Toriumi A 2008 *Applied Physics Express* **1** 51406 URL http://dx.doi.org/10.1143/APEX.1.051406

[29] Schubert E F 1990 *Journal of Vacuum Science {&} Technology A: Fundamentals and device applications* **8** 2980 URL http://dx.doi.org/10.1116/1.576617

[30] Gossmann H J and Schubert E F 1993 *Critical Reviews in Solid State and Materials Sciences* **18** 1–67 URL http://dx.doi.org/10.1080/10408439308243415

[31] Goh K E J, Oberbeck L, Simmons M Y, Hamilton A R and Butcher M J 2006 *Physical Review B - Condensed Matter and Materials Physics* **73** 1–6 ISSN 10980121 URL http://dx.doi.org/10.1103/PhysRevB.73.035401

[32] Sze S M 1981 *Physics of Semiconductor Devices* Wiley-Interscience publication (John Wiley & Sons) ISBN 9780471056614

[33] Olikh O Y 2015 *Journal of Applied Physics* **118** 24502 URL http://dx.doi.org/0.1063/1.4926420

[34] Gromov D and Pugachevich V 1994 *Applied Physics A* **59** 331–333 URL http://dx.doi.org/10.1007/BF00348239

[35] Mead C A 1966 *Solid-State Electronics* **9** 1023–1033 URL http://dx.doi.org/10.1016/0038-1101(66)90126-2

[36] Card H C and Rhoderick E H 1971 *Journal of Physics D: Applied Physics* **4** 1589 URL http://dx.doi.org/10.1088/0022-3727/4/10/319

[37] Werner J H and Gijttler H H 1991 *Journal of Applied Physics* **69** 1522 URL http://dx.doi.org/10.1063/1.347243

[38] Allen P B and Cardona M 1983 *Physical Review B* **27** 4760–4769 URL http://dx.doi.org/10.1103/PhysRevB.27.4760

[39] Lautenschlager P, Allen P B and Cardona M 1985 *Physical Review B* **31** 2163–2171 URL http://dx.doi.org/10.1103/PhysRevB.31.2163

[40] Tung R T 1992 *Physical Review B* **45** 13509 URL http://dx.doi.org/10.1103/PhysRevB.45.13509

[41] Tung R T, Sullivan J P and Schrey E 1992 *Materials Science {&} Engineering B* **14** 266–280 URL http://dx.doi.org/10.1016/0921-5107(92)90309-W

[42] Saxena A N 1969 *Surface Science* **13** 151–171 URL http://dx.doi.org/10.1016/0039-6028(69)90245-3

[43] Johnson V A, Smith R N and Yearian H J 1950 *Journal of Applied Physics* **21** 283–289 ISSN 00218979 URL http://dx.doi.org/10.1063/1.1699654

[44] Song Y P and RL Van Meirhaeghe, WH Laflère F C 1986 *Solid-State Electronics* **29** 633–638 URL http://dx.doi.org/10.1016/0038-1101(86)90145-0

[45] Chand S and Kumar J 1996 *Semiconductor Science and Technology* **11** 1203 ISSN 0268-1242 URL http://dx.doi.org/10.1088/0268-1242/21/3/016

[46] Mamor M 2009 *Journal of Physics: Condensed Matter* **21** 335802 URL http://dx.doi.org/10.1088/0953-8984/21/33/335802

[47] Gülnahar M and Efeolu H 2009 *Solid-State Electronics* **53** 972–978 ISSN 00381101 URL http://dx.doi.org/10.1016/j.sse.2009.03.027

[48] Spiesser A, Virot F, Michez L A, Hayn R, Bertaina S, Favre L, Petit M and Le Thanh V 2012 *Physical Review B* **86** 035211 ISSN 1098-0121 URL http://dx.doi.org/10.1103/PhysRevB.86.035211

[49] Truong A, Watanabe A O, Mortemousque P A, Ando K, Sato T, Taniyama T and Itoh K M 2015 *Physical Review B* **91** 214425 ISSN 1098-0121 URL http://dx.doi.org/10.1103/PhysRevB.91.214425

[50] Scappucci G, Capellini G, Lee W C T and Simmons M Y 2009 *Applied Physics Letters* **94** 162106 ISSN 00036951 URL http://dx.doi.org/10.1063/1.3123391

[51] Chroneos A, Bracht H, Grimes R W and Uberuaga B P 2008 *Materials Science and Engineering B: Solid-State Materials for Advanced Technology* **154-155** 72–75 ISSN 09215107 URL http://dx.doi.org/10.1016/j.mseb.2008.08.005

[52] Hartmann J M, Barnes J P, Veillerot M, Fédéli J M, Benoit A La Guillaume Q and Calvo V 2012 *Journal of Crystal Growth* **347** 37–44 ISSN 00220248 URL http://dx.doi.org/10.1016/j.jcrysgro.2012.03.023

[53] Padovani F A and Sumner G G 1965 *Journal of Applied Physics* **36** 3744–3747 ISSN 00218979 URL http://dx.doi.org/10.1063/1.1713940

[54] Padovani F A and Stratton R 1966 *Solid-State Electronics* **9** 695–707 ISSN 00381101 URL http://dx.doi.org/10.1016/0038-1101(66)90097-9

[55] Horváth Z, Bosacchi A, Franchi S, Gombia E, Mosca R and Motta A 1994 *Materials Science {&} Engineering B* **28** 429–432 URL http://dx.doi.org/10.1016/0921-5107(94)90099-X

[56] Yamada M, Sawano K, Uematsu M and Itoh K M 2015 *Applied Physics Letters* **107** 1–5 ISSN 00036951 URL

http://dx.doi.org/10.1063/1.4931939